

## Supporting Information

# Effects of SiO<sub>2</sub> sub-supporting layer on the structure of Al<sub>2</sub>O<sub>3</sub> supporting layer, formation of Fe catalyst particles, and growth of carbon nanotube forests

*Jaegun Lee,<sup>1</sup> Cheol Hun Lee,<sup>2</sup> Junbeom Park,<sup>2</sup> Dong Myeong Lee,<sup>1</sup> Kun-Hong Lee,<sup>2</sup> Sae Byeok Jo,<sup>2</sup> Kilwon Cho,<sup>2</sup> Benji Maruyama,<sup>3</sup> and Seung Min Kim<sup>1,\*</sup>*

<sup>1</sup>Institute of Advanced Composite Materials, Korea Institute of Science and Technology, 92, Chudong-ro, Bongdong-eup, Wanju-gun, Jeollabuk-do, South Korea 55324

<sup>2</sup>Department of Chemical Engineering, Pohang University of Science & Technology, 77 Cheongam-Ro, Nam-Gu, Pohang, Gyeongbuk, South Korea 37673

<sup>3</sup>Materials and Manufacturing Directorate, Air Force Research Laboratory, Wright-Patterson Air Force Base, OH 45433

---

\*Corresponding author. Tel : +82-63-219-8154

E-mail address: seungmin.kim@kist.re.kr (S. M. Kim)

## 1. Characterization of CNT forests

With both cases of the catalyst configurations, there is no significant difference in the heights of CNT forests and diameters of the CNTs. The heights of CNT forests grown for 3 minutes are about 400  $\mu\text{m}$  for both catalyst configurations. The CNTs are multi-walled and have average diameter of 12 nm. The CNT forest grown on Fe 1 nm/ $\text{Al}_2\text{O}_3$  10 nm/ $\text{SiO}_2$  300 nm/Si(100) wafer for 3-10 min is usually spinnable, even though longer growth time degrades the spinnability.

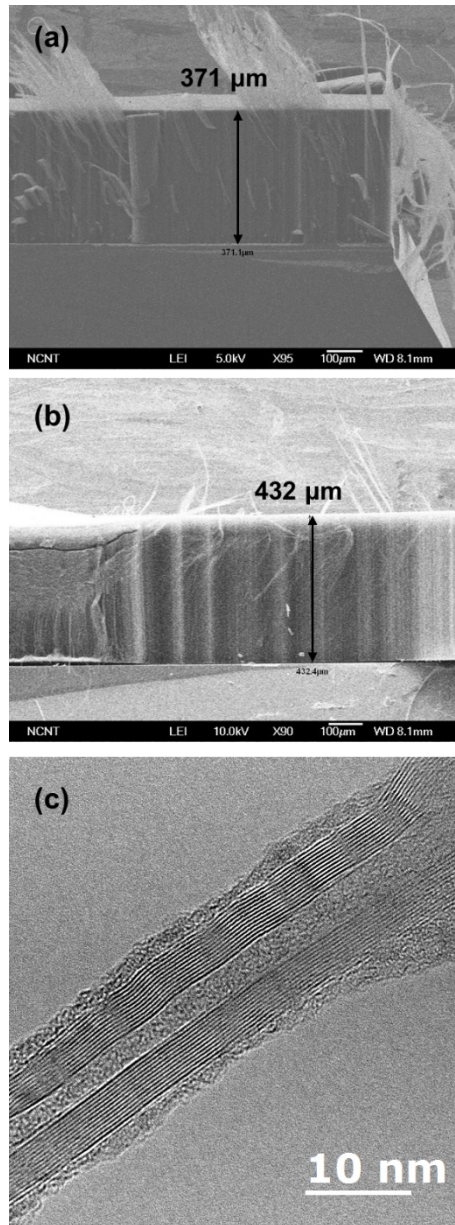


Figure S1. Low magnification SEM images of CNT forests grown on (a) Fe 1 nm/ $\text{Al}_2\text{O}_3$  10 nm/Si and (b) Fe 1 nm/ $\text{Al}_2\text{O}_3$  10 nm/ $\text{SiO}_2$  300 nm/Si wafers. (c) A TEM image of a typical CNT from the CNT forests.

## 2. Comparison of the porosity of Al<sub>2</sub>O<sub>3</sub> films by TEM image

As shown in Figure S2, it is very difficult to obtain any quantitative information about the porosity of the alumina films from high-resolution TEM images. Thus, in our work, the ellipsometry technique was used to evaluate the porosity of alumina films.

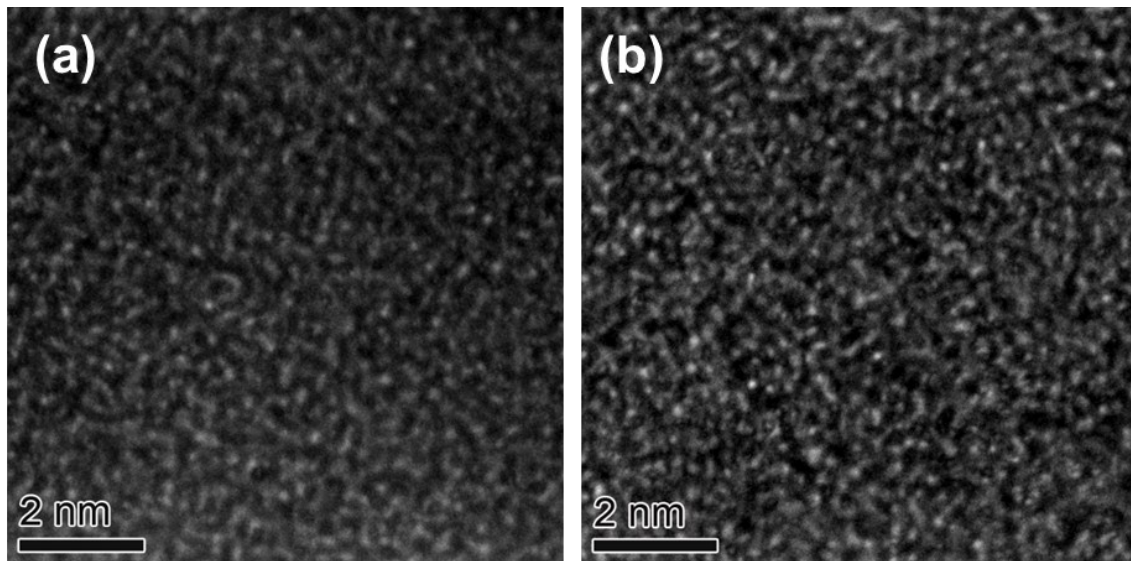


Figure S2. High-resolution TEM images of Al<sub>2</sub>O<sub>3</sub> support layers (a) without and (b) with thermally grown SiO<sub>2</sub> sub-supporting layer.

### 3. Elemental analysis

To confirm the composition of the  $\text{Al}_2\text{O}_3$  films on Si wafer and  $\text{SiO}_2/\text{Si}$  wafer are identical, TEM-EDS analyses were performed. As shown in Figure S3(c), the atomic ratios of Al and O are nearly identical in  $\text{Al}_2\text{O}_3$  layer of the two substrates.

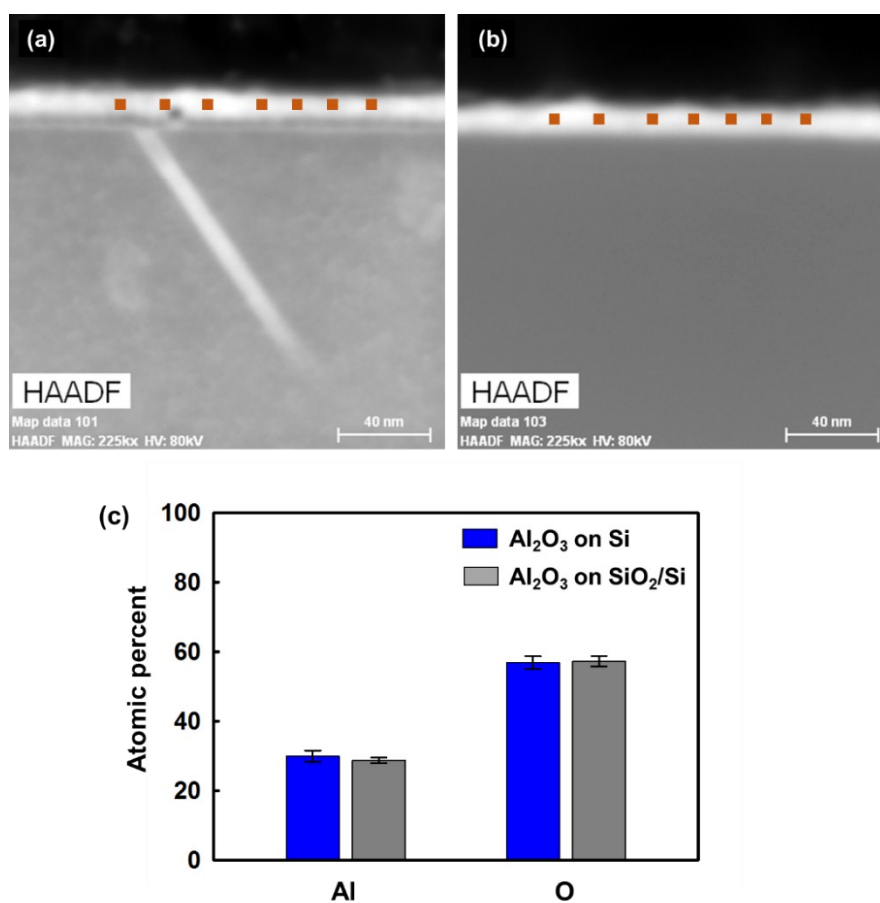


Figure S3. HAADF STEM images of (a)  $\text{Fe}/\text{Al}_2\text{O}_3/\text{Si}$  wafer and (b)  $\text{Fe}/\text{Al}_2\text{O}_3/\text{SiO}_2/\text{Si}$  wafer. Red dots in (a) and (b) indicate seven positions where elemental analysis was taken. (c) Average atomic percent of Al and O of  $\text{Al}_2\text{O}_3$  layers from atomic percent at the seven positions in Figure S3(a) and (b).

#### 4. Role of SiO<sub>2</sub> as diffusion barrier (X-ray diffraction, TEM)

Two high-resolution TEM images are added to clearly show the interface between Al<sub>2</sub>O<sub>3</sub> and SiO<sub>2</sub> layer. No additional phase is observed at the interface of the whole sample.

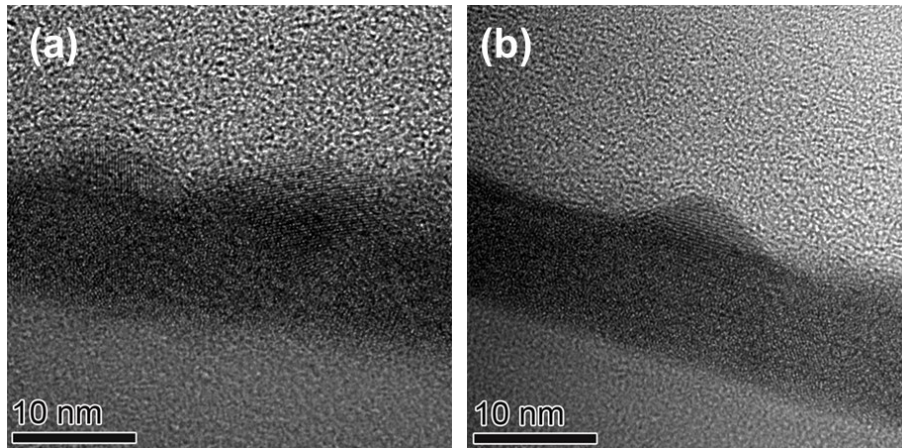


Figure S4. High-resolution TEM images of the interface between Al<sub>2</sub>O<sub>3</sub> and SiO<sub>2</sub> layers.

The crystallinity of heat-treated wafer was characterized using X-ray diffractometer (Rigaku, Smartlab). No crystalline structure other than Si is observed, which is in consistence with the TEM images shown in Figure 4(b), Figures 7(a) and 7(b).

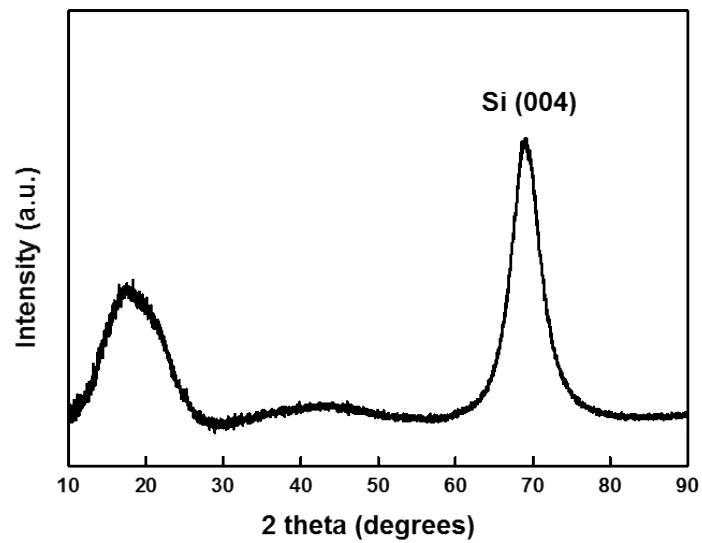


Figure S5. XRD pattern of Fe 1 nm/Al<sub>2</sub>O<sub>3</sub> 10 nm/SiO<sub>2</sub> 300 nm/Si wafer after heat-treating at 700 °C under H<sub>2</sub> atmosphere for 10 min.